Accurate stress fields of post-buckled laminated composite beams accounting for various kinematics

Electrochemical corrosion behaviour of binary magnesium - heavy rare earth alloys

F. Rosalbino, S. De Negri, G. Scavino, A. Saccone

The corrosion properties of magnesium-heavy rare earth (RE) based alloys have been studied. Binary additions of gadolinium (Gd), dysprosium (Dy) and erbium (Er) to pure magnesium were made to a nominal 1 at.%. The corrosion resistance of Mg99Gd1, Mg99Dy1 and Mg99Er1 alloys has been assessed by using open circuit potential measurements, potentiodynamic polarization curves and electrochemical impedance spectroscopy (EIS) carried out in 0.075 M Na2B4O7 + 0.05 M H3BO3 solution, pH = 8.4. Electrochemical results showed that heavy RE alloying additions significantly improves the corrosion behaviour of magnesium. This improvement can be attributed to enhanced barrier properties of the corrosion products layer and additional active corrosion protection originated from the inhibiting action of the lanthanide cations entrapped as oxides/hydroxides in this surface layer.

KEYWORDS: MAGNESIUM; HEAVY RARE EARTH; CORROSION; POLARIZATION; ELECTROCHEMICAL IMPEDANCE SPECTROSCOPY

INTRODUCTION

Magnesium alloys constitute a very interesting alternative to the materials traditionally applied in structural applications, and, especially in the automotive and aircraft industry. The main advantage of magnesium alloys is the reduction of the weight of the components due to the low density and high specific strength of these materials [1, 2]. However, the principal drawback of magnesium alloys is the low corrosion resistance, which is generally, much lower when compared to many other competing materials, like aluminum alloys or steels [2]. This limits the range of technical applications of these materials.

The stability of several metals and alloys depends upon the formation of stable surface films. However, in magnesium and its alloys the surface film that forms spontaneously is poorly protective and very unstable in a wide range of pH values. This film becomes protective and stable only at pH values over 11 [3].

Literature reporting the electrochemical behavior of pure magnesium [4 - 7], zirconium free [8 - 14] and zirconium containing alloys [15 - 19], has been published in the last decade. Improvements to the corrosion resistance of Mg alloys have been correlated with the addition of alloying elements such as aluminum [8, 11 - 13], zirconium [16 - 18] and yttrium [19].

Addition of rare earths (RE) as alloying elements to the solid phase is an effective way to enhance the corrosion behavior of magnesium alloys. The scavenger effect, optimized microstructure and formation of more protective corrosion product films were considered as the main key factors to improve the corrosion resistance of RE-containing Mg alloys surface and to the inhibition of further corrosion [20 - 23]. However, it has also been suggested that the oxidation of the RE, followed by an enrichment of these elements in the surface film, decreases the corrosion rate by forming a pseudo passive layer [24]. Moreover, It has been reported [11] that the oxides formed can be more compact and able to trap harmful anions by making the surface charge more positive.

The objective of this work is to contribute to a better under-

F. Rosalbino, G. Scavino
Dipartimento di Scienza Applicata e Tecnologia, Politecnico di Torino, Corso Duca degli Abruzzi, 24 – 10129 Torino (Italy)

S. De Negri, A. Saccone
Università degli Studi di Genova, Dipartimento di Chimica e Chimica Industriale, Via Dodecaneso 31 – 16146 Genova (Italy)

standing of the corrosion mechanism of magnesium alloys and especially the role of heavy rare earths in buffer neutral/alkaline solution. The electrochemical corrosion behaviour of binary Mg-RE alloys containing gadolinium (Gd), dysprosium (Dy) and erbium (Er), was assessed and compared with that of unalloyed magnesium in order to gain information about the influence of the heavy RE on corrosion process. The corrosion behaviour of the RE-containing Mg alloys was investigated by using open circuit potential measurements, potentiodynamic polarization curves and electrochemical impedance spectroscopy (EIS) carried out in borate buffer solution. This electrolyte allows for an insight into the role of the RE in the corrosion mechanism by imposing a pH at which Mg can cover itself with scarcely protective oxide or hydroxide which checks the dissolution reaction [3]. Furthermore, the buffering effect avoids pH fluctuations, which in NaCl solutions, for example, may increase more than 4 units.

Experimental

Binary alloys with nominal composition Mg99RE1 (at.%, RE = Gd, Dy, Er) were prepared by direct synthesis from the constituent metals (purity > 99.9 mass %, Mg was supplied by MaTecK, Jülich,Germany, the rare earth metals by Newmet Koch, Waltham Abbey, England). Stoichiometric amounts of the elements were enclosed in arc-sealed Ta crucibles, in order to prevent Mg losses due to evaporation, and induction melted under argon flow. Melting was repeated three times in order to ensure homogeneity. Ingots with a diameter of ~0.8 cm and a mass of ~0.4 g were extracted from the crucibles after quenching in cold water. Chemical composition of samples was determined by spectrometric analysis employing an argon microwave plasma torch coupled to spark ablation (Spectro Analytical Instruments). Specimens were ablated by a medium voltage spark (450 V, 370 Hz) in a point-to-plane configuration (spark times: 125 s) and swept into a 100-W, 2.45-GHz argon microwave discharge. The microwave plasma was observed end-on and the radiation analyzed with a polychromator.

Microstructure examination was performed by a scanning electron microscope (SEM) Zeiss Evo 40 equipped with a Pentafet Link Energy Dispersive X-ray Spectroscopy (EDXS) system managed by the INCA Energy software (Oxford Instruments, Analytical Ltd., Bucks, U.K.). Smooth surfaces for microscopic observation before the electrochemical tests were prepared by using SiC papers and diamond pastes with grain size down to 1 µm.

All the electrochemical tests were carried out in a single compartment cell using a standard three electrode configuration: saturated calomel electrode (SCE) as a reference with a platinum electrode as counter and a sample as the working electrode. The surface area exposed to the test solution was 0.5 cm2. Before each measurement, the samples surface was first ground with 320, 400 and 600 µm SiC abrasive papers in anhydrous ethyl alcohol and then automatically polished up to 1 µm using diamond pastes and non aqueous lubricants until a mirror-bright surface was achieved. All the experiments were performed at room temperature (25 ± 0.1 °C) in naturally aerated sodium borate/boric acid buffer solution of pH 8.4. The p.a. reagents (0.075 M $Na_2B_4O_7$ and 0.05 M H_3BO_3) were added in Millipore® water.

Potentiodynamic polarization curves were recorded starting from -2400 mV/SCE and moving in the electropositive direction at a scan rate of 1 mV/s, after allowing a steady-state potential to develop. Free corrosion potential was recorded with respect to the SCE every minute for a period of 2 h. All stationary measurements were carried out using an Amel System 5000 potentiostat controlled by a personal computer.

Electrochemical impedance was measured at the open circuit potential using a Gamry FAS2 Femtostat with a PC4 Controller. The frequency range analyzed went from 100 kHz up to 10 mHz, with the frequency values spaced logarithmically (seven per decade). The width of the sinusoidal voltage signal applied to the system was 10 mV rms (root-mean-square). Impedance measurements were performed at different exposure times in the electrolyte.

For comparison, the electrochemical tests were also performed on unalloyed magnesium, supplied by Johnson Matthey, London, UK.

SEM-EDXS were used to investigate morphology and chemical composition of specimens surface after the electrochemical tests.

Results and discussion

Representative SEM micrographs of the Mg – heavy RE alloys are shown in Figure 1. All tested alloys are basically constituted by a Mg-based matrix, where the rare earth is totally dissolved, giving an average concentration near to the nominal one. In all specimens the magnesium solid solution is the only detected phase. The obtained results are in agreement with the solubility trend of the rare earth metals in magnesium, increasing from Gd to Er [18]. Moreover, the presence of small isolated particles is also detected. These particles may have formed during the melting process and typically contains Mg and O, as estimated using EDXS analysis.

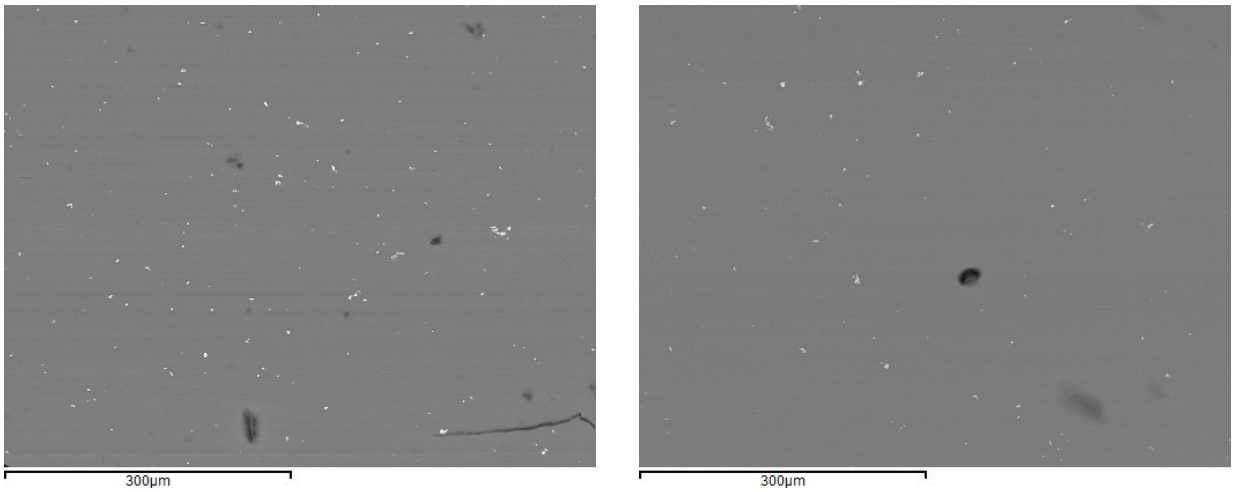

Fig. 1 - Representative SEM micrographs of $Mg_{99}RE_1$ alloys. (a) $Mg_{99}Gd_1$ alloy; (b) $Mg_{99}Er_1$ alloy (single phase samples)

Figure 2 reports the open circuit potential, E_{OC}, of unalloyed Mg and $Mg_{99}RE_1$ alloys in naturally aerated sodium borate/boric acid buffer solution, monitored for 2 h. The open circuit potential provides some indication of the reactivity of the metal surface. As can be seen, the open circuit potential of each $Mg_{99}RE_1$ alloys and for unalloyed Mg is, as expected, relatively negative immediately after the specimen is immersed in the solution, and subsequently the open circuit potential gradually shifts towards more positive values. This positive shift can be attributed to deposition of corrosion products on the sample surface. By comparing the results reported in Figure 2, it can be observed that the open circuit potential of $Mg_{99}RE_1$ alloys is less negative than that recorded on unalloyed Mg. This behaviour indicates that the corrosion products layer formed at the surface of $Mg_{99}RE_1$ alloys displays better corrosion protection characteristics than the one formed on unalloyed magnesium in 0.075 M $Na_2B_4O_7$ + 0.05 M H_3BO3 solution.

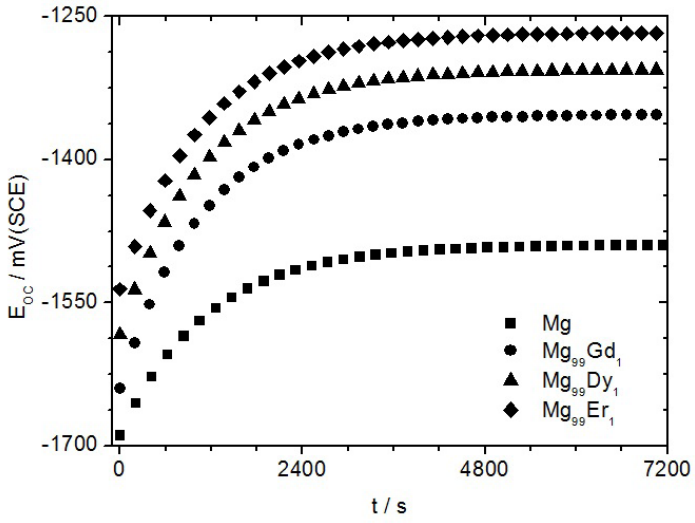

Fig. 2 - Variation of the open circuit potential, E_{OC}, with exposure time in naturally aerated 0.075 M $Na_2B_4O_7$ + 0.05 M H_3BO_3 solution, pH = 8.4, for unalloyed Mg and $Mg_{99}RE_1$ alloys

Figure 3 shows typical polarization curves of unalloyed Mg and $Mg_{99}RE_1$ alloys recorded in naturally aerated sodium borate/boric acid buffer solution at 25 °C. As can be seen, the shapes of the polarization curves are similar indicating similar corrosion mechanisms. One important feature is that the presence of heavy RE provokes a significant shift in the corrosion potential to more positive values as compared to unalloyed Mg, thereby confirming the previous E_{OC} measurements. The anodic response for all specimens is characterized by activation controlled kinetics in the vicinity of the corrosion potential. In fact, the anodic current densities initially increase exponentially with increasing potential above E_{corr}. However, as the potential becomes more anodic, the behaviour is no longer exponential and all samples reach a maximum current density after which the current density gradually drops with further increasing potential. The potential where the current density peaks to a maximum is known as the passivation potential, E_{pass}, while the current at this potential is referred to as the critical current density, icc. For unalloyed Mg, the E_{pass} value is −1150 mV/SCE and the i_{cc} value is 4.7 mA cm^{-2}. Regarding $Mg_{99}RE_1$ alloys, the passivation potential is shifted towards more noble values, while the critical current density exhibits lower values. On further scanning in the anodic direction the current density remains independent of potential and a well-defined plateau appears thereby indicating the onset of a *pseudopassivation* process attributable to formation of a corrosion product layer at the surface of corroding sample [26 - 30]. This current is known as the pseudopassivation current density, i_{pp}. As can be observed in Figure 3 the ipp value of unalloyed Mg is 2.6 mA cm^{-2} while the pseudopassive region extends from about −1150 to 1490 mV/SCE when the surface layer begins to break down in the solution employed and the anodic current density rises again. The presence of rare earths improves the pseudopassivation behaviour, resulting in a larger pseudopassive region extending from about −930 to 1780 mV/SCE for $Mg_{99}Gd_1$ alloy, from about −910 to 1840 mV/SCE for $Mg_{99}Dy_1$ alloy and from −880 to 1920 mV/SCE for $Mg_{99}Er_1$ alloy. The electrochemical parameters deduced from the analysis of the anodic part of the polarization curves recorded in 0.075 M $Na_2B_4O_7$ + 0.05 M H_3BO_3 solution are summarized in Table 1. As was previously shown, heavy RE alloying additions increase the extent, ΔE, of the pseudopassive region, thereby indicating the formation of a more stable surface layer on $Mg_{99}RE_1$ electrodes. Moreover, the RE-containing Mg alloys show pseudo-passive current density values lower than that of unalloyed Mg, suggesting that the corrosion products layer formed on these systems exhibits better protective characteristics.

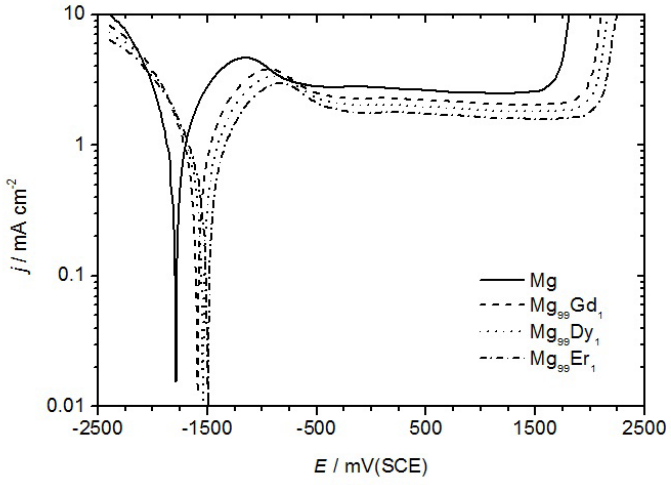

Fig. 3 - Potentiodynamic polarization curves for unalloyed Mg and $Mg_{99}RE_1$ alloys in naturally aerated 0.075 M $Na_2B_4O_7$ + 0.05 M H_3BO_3 solution, pH = 8.4

Tab. 1 - Electrochemical parameters obtained from the potentiodynamic polarization curves of unalloyed Mg and $Mg_{99}RE_1$ alloys recorded in naturally aerated $Na_2B_4O_7$ + 0.05 M H_3BO_3 solution, pH = 8.4

Sample	E_{corr} (mV/SCE)	E_{pass} (mV/SCE)	i_{cc} (mA cm^{-2})	ΔE (mV)	i_{pp} (mA cm^{-2})
Mg	-1790	-1150	4.70	2640	2.60
$Mg_{99}Gd_1$	-1590	-930	3.90	2710	2.20
$Mg_{99}Dy_1$	-1530	-880	3.40	2750	1.90
$Mg_{99}Er_1$	-1480	-830	2.90	2800	1.60

E_{corr} = Corrosion potential; **E_{pass}** = passivation potential; **i_{cc}** = critical current density; **ΔE** = pseudopassive range; **i_{pp}** = pseudopassivation current density

In order to obtain e deeper understanding of the corrosion processes, electrochemical impedance spectra (EIS) were measured at hourly intervals for $Mg_{99}RE_1$ and unalloyed Mg at the corrosion potential during 24 h exposure to $Na_2B_4O_7$ + 0.05 M H_3BO_3 solution. The surfaces were examined at the end of each experiment using scanning electron microscopy coupled with EDXS analysis.

Figure 4 shows the evolution of the impedance diagrams, in the form of Nyquist plots, for unalloyed Mg and $Mg_{99}RE_1$ alloys a function of exposure time to naturally aerated sodium borate/boric acid buffer solution. The EIS spectra are similar in all cases and changes in a similar manner with increasing exposure time. The Nyquist plots are characterized by two well-defined capacitive loops: a high to medium frequency (HF) and a medium to low frequency (MF) capacitive loop, as labelled. The diameter of the HF capacitive loop typically represents the charge transfer resistance (R_{ct}) of an actively corroding electrode, with determined capacitance values consistent with the electrochemical double layer. The MF capacitive loop is attributed to the presence of the surface film influencing the corrosion process. In this case, the charge transfer resistance through this defective (porous) surface layer is not much higher than for the processes occurring on the bare surface of specimen. The corrosion can be designed as active dissolution in both cases. The difference is in the different dielectric properties of this surface film, inducing higher capacitance values.

The polarization resistance, R_p, is evaluated in this case of poor surface stability as the distance from the impedance values at the highest frequency (theoretically at infinite frequency) to the impedance at the lowest frequency (f = 0.01 Hz) determined on the real part of impedance coordinate in the Nyquist plot. The polarization resistance is related to the corrosion resistance and the corrosion rate; high values of polarization resistance relate to high corrosion resistance and to low corrosion rates. The increasing size of the HF loop typically indicates lateral stabilization of the surface layer resulting in a decreasing actively dissolving surface and as a consequence an higher impedance. For unalloyed Mg and $Mg_{99}RE_1$ alloys, there is an increase of polarization resistance, indicating that the corrosion resistance increases (attributed to an increased stability of the defective surface product layer).

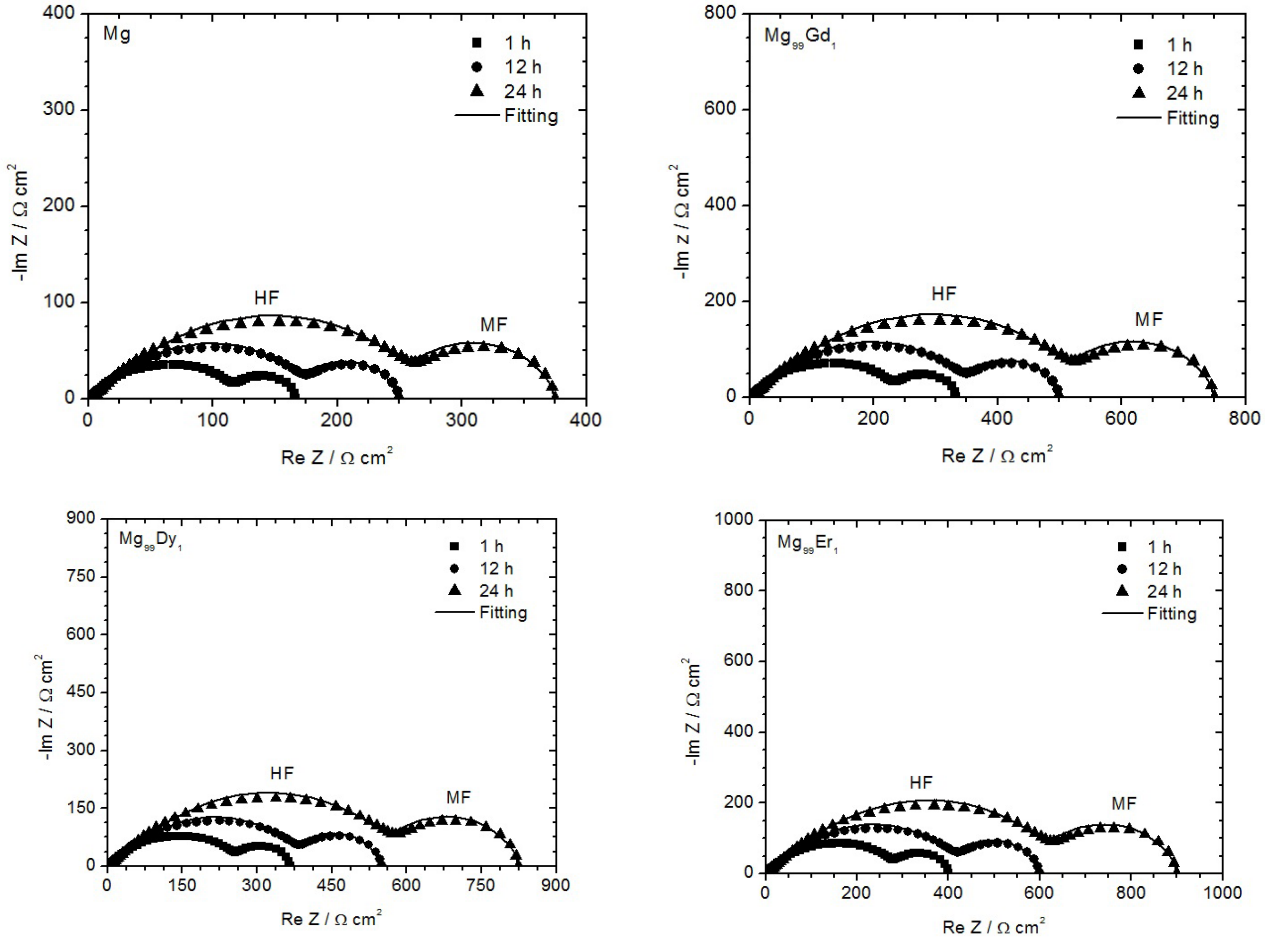

Fig. 4 - Representative Nyquist diagrams of unalloyed Mg and $Mg_{99}RE_1$ alloys for various exposure times to naturally aerated 0.075 M $Na_2B_4O_7$ + 0.05 M H_3BO_3 solution, pH = 8.4

Figure 5 presents the polarization resistance, R_p, versus exposure time as measured from the Nyquist plots. In all cases the polarization resistance (and the corrosion resistance) increases with increasing exposure time, suggesting that a surface corrosion products layer grows on the electrode surface and that this layer effectively slows down active corrosion. As can be seen, $Mg_{99}RE_1$ alloys exhibit higher values of R_p as compared to unalloyed Mg, thereby indicating that the magnesium charge transfer process is significantly inhibited by the alloyed heavy rare earth elements because of the formation of a more protective surface film which develops an effective barrier against corrosion, in agreement with the results obtained from open circuit potential and potentiodynamic polarization measurements (Figs. 2, 3).

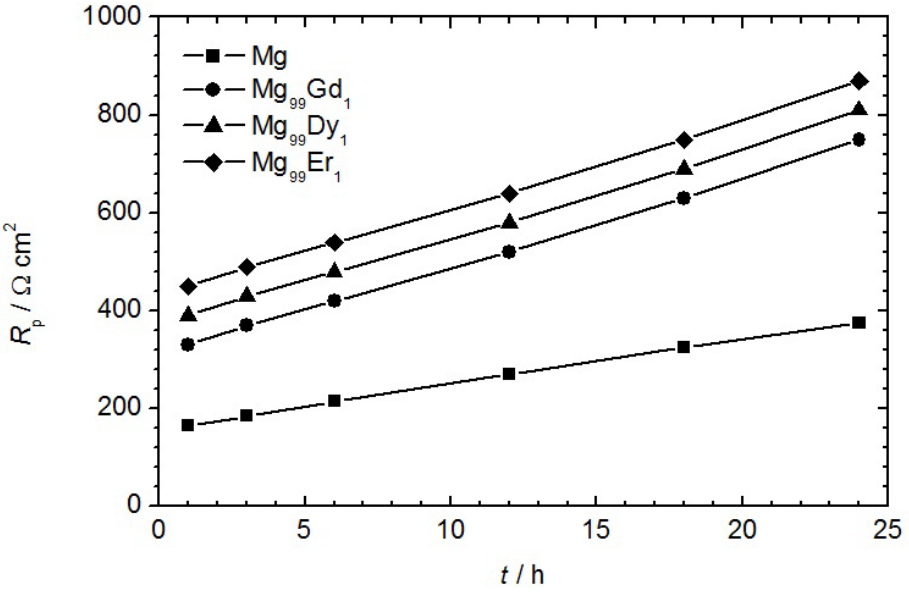

Fig. 5 - Variation of polarization resistance, R_p, for unalloyed Mg and $Mg_{99}RE_1$ alloys as a function of exposure time to naturally aerated 0.075 M $Na_2B_4O_7$ + 0.05 M H_3BO_3 solution, pH = 8.4

SEM-EDXS characterization of samples surface at the end of each EIS experiment was carried out in order to gain information about the composition and morphology of corrosion products layer which plays an important role in determining the corrosion behaviour of investigated materials. The different solid corrosion products, formed on their surface at the onset of dissolution, may hinder the transportation of the corrosion medium as well as the mass exchange of reagents.

Representative SEM micrographs of unalloyed Mg and Mg99RE1 alloys after 24 h exposure to naturally aerated 0.075 M $Na_2B_4O_7$ + 0.05 M H_3BO_3 solution are shown in Figure 6. A corrosion products layer covers the entire surface of all specimens.

A thin oxide/hydroxide film forms spontaneously at the surface of Mg on exposition to ambient air [31, 32]. This surface film is not compact and part of the Mg substrate can be easily exposed. In an aqueous solution, the Mg surface film is covered by a thick porous layer of $Mg(OH)_2$. The dissolution reaction mainly occurs at the bare parts of the Mg surface, and can be summarized [4, 33 - 35] as follows. The corrosion of Mg converts metallic Mg to the stable ion, Mg^{++}, in two electrochemical steps, (2) and (3). These anodic reactions are balanced by the cathodic partial reaction (1). The uni-positive ion, Mg^+, is so reactive that it has never been detected [33]. The overall reaction is (4).

$2H_2O + 2e^- \rightarrow 2OH^- + H2$ cathodic reaction (1)
$Mg \rightarrow Mg^+ + e^-$ anodic reaction (2)
$Mg^+ \rightarrow Mg^{++} + e^-$ anodic reaction (3)
$Mg + 2H_2O \rightarrow Mg(OH)_2 + H_2$ overall reaction (4)

EDXS analysis performed on the surface layer of $Mg_{99}RE_1$ alloys also evidenced a significant amount of rare earth metals (about 5 at.%) in the form of oxide/hydroxide. The lanthanide cations formed during dissolution of alloy (reaction (5)) react with the hydroxyl ions (reaction (1)) giving rise to an insoluble oxide/hydroxide film that precipitates at the alloy surface (reactions (6) and (7)) [36, 37]:

$RE \rightarrow RE^{3+} + 3e^-$ (5)
$RE^{3+} + OH^- \rightarrow RE(OH)_3$ (6)
$2RE(OH)_3 \rightarrow RE_2O_3 + 3H_2O$ (7)

Gd_2O_3, Dy_2O_3 and Er2O3 are insoluble in water. The solubility product constants, K_{sp}, for $Gd(OH)_3$, $Dy(OH)_3$ and $Er(OH)_3$ are 1.1×10^{-22}, 1.4×10^{-22} and 1.8×10^{-22}, respectively, which are much smaller than that of $Mg(OH)_2$ (5.61×10^{-12}). Thus Gd_2O_3, Dy_2O_3 or Er_2O_3 and $Gd(OH)_3$, $Dy(OH)_3$ or $Er(OH)_3$ are more likely to be retained in the corrosion products layer than $Mg(OH)_2$, due to the lower solubility. This results in the enrichment of Gd, Dy or Er in the corrosion products layer. The presence of rare earth oxide/hydroxide film may explain the differences between the surface morphology of pure Mg (Fig. 6a), on one hand, and that of rare earth-containing alloys, on the other, evidenced by SEM observations (Fig. 6b-d).

Literature reports improved corrosion resistance of magnesium alloys exposed to aggressive environments containing lanthanide ions [38]. This improvement was attributed to the precipitation of a protective film of rare

earth oxides/hydroxides on the cathodic sites. Hybrid silica sol-gel coatings containing lanthanide ions formed on pure magnesium and on magnesium alloys were also tested [39, 40]. It was reported that the sol-gel film modified with rare earths behave as conversion coatings on the metallic substrates. The anticorrosive performance of lanthanide ions entrapped in the hybrid silica sol-gel network occurs by means of the inhibitor effect and self-repairing mechanism (probably associated with rare $RE(OH)_3$ precipitation) [40].

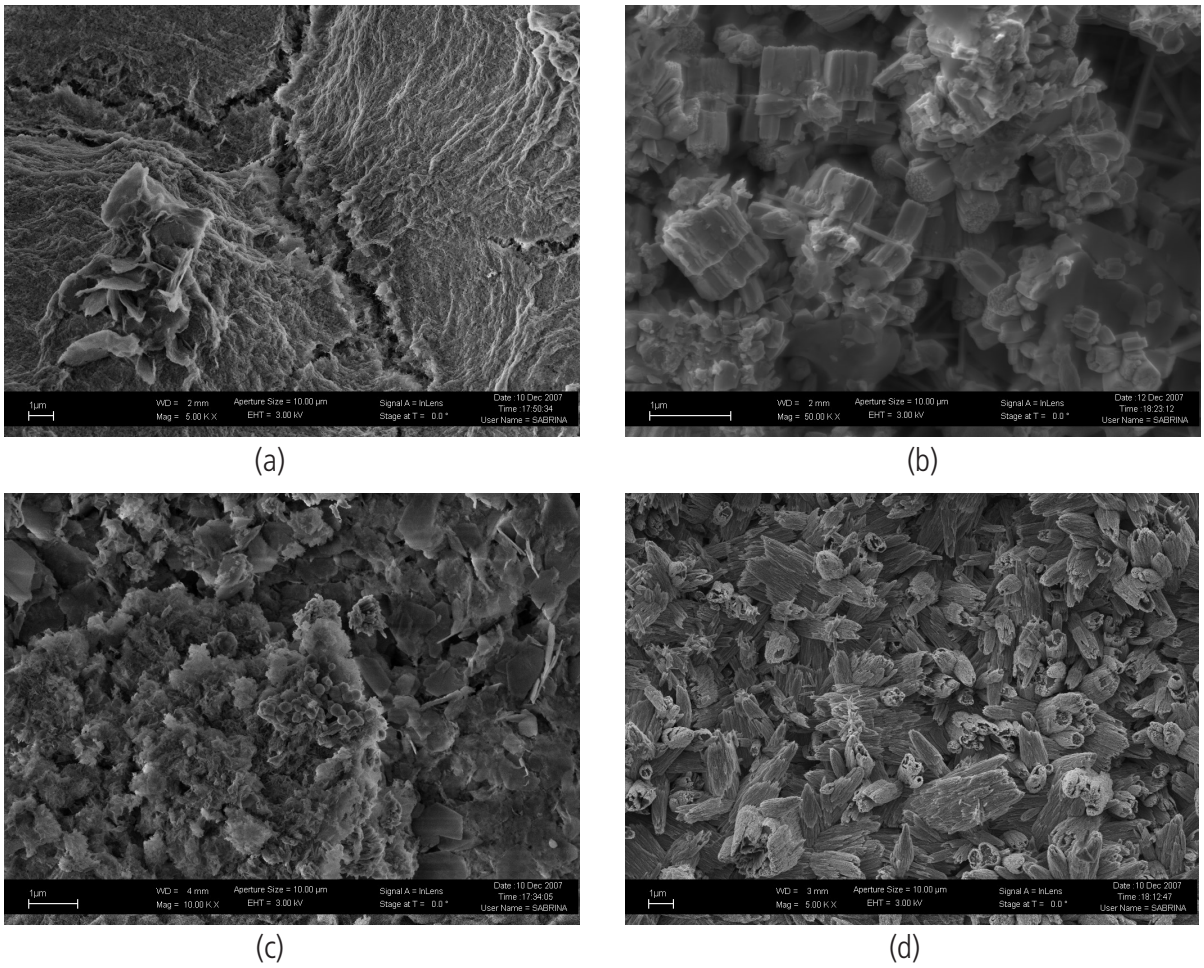

Fig. 6 -Representative SEM micrographs of the corrosion products layer formed at the surface of pure Mg (a); $Mg_{99}Gd_1$ alloy (b); $Mg_{99}Dy_1$ alloy (c); $Mg_{99}Er_1$ alloy (d) after 24 h exposure to naturally aerated 0.075 M $Na_2B_4O_7$ + 0.05 M H_3BO_3 solution, pH = 8.4

The d.c. polarization and EIS results obtained in the present work show significant improvement of the corrosion behaviour of $Mg_{99}RE_1$ alloys in sodium borate/boric acid buffer solution with respect to unalloyed magnesium. This result is linked with the presence of a more stable surface layer responsible for the higher R_p and lower i_{pp} values compared to unalloyed Mg. Since the negative electrochemical potential of the elements Gd, Dy and Er [41], is very similar to that of the element Mg, elemental RE does not cause micro-galvanic corrosion of the Mg matrix. Moreover, RE dissolved in the Mg matrix increases the protective nature of the surface film as evidenced for Mg-Y alloys [42, 43]. The incorporation of oxidized Y in the surface film was identified as enhancing their degradation resistance. Therefore, Gd, Dy and Er, in the oxidized state, can incorporate in the surface layer, increase its protectiveness and thereby decrease the corrosion progress of metallic substrate. Since rare earth oxides/hydroxides are very insulating they may contribute to enhance the dielectric properties of the corrosion products layer, thus reinforcing its barrier properties. Besides, rare earths alloying addition to pure Mg may impart active corrosion protection properties to the corrosion products layer, further improving its protection ability. Additional active corrosion protection originates from an inhibiting action of the rare earth cations, RE^{3+}, entrapped as oxides/hydroxides in the corrosion products layer. This surface layer hinders the mass exchange of reagents and products between the substrate and the corrosive medium, thus impeding further degradation and consequently increasing the corrosion resistance. Similar explanation was also proposed in literature [40] to interpret the improved corrosion protection of sol-gel film containing La, Ce and Pr.

Further investigation is planned aiming at a deeper understanding of the protective behaviour of these surface layers.

Conclusions

The corrosion behaviour of $Mg_{99}RE_1$ alloys in naturally aerated sodium borate/boric acid buffer solution has been assessed and compared with that of unalloyed magnesium. The following conclusions can be drawn:

1. Addition of heavy the rare earth elements Gd, Dy and Er significantly improves the corrosion resistance of magnesium.
2. The increased corrosion stability of $Mg_{99}RE_1$ alloys is ascribed to the formation of a "lanthanide-doped" corrosion products layer (magnesium hydroxide, $Mg(OH)_2$), which exhibits higher stability with respect to that formed on unalloyed Mg (higher R_p and lower i_{pp} values).
3. SEM-EDXS characterization of the corrosion products layer present at the surface of $Mg_{99}RE_1$ alloys evidenced significant amounts of rare earth in the form of oxide/hydroxide. RE elements, in the oxidized state, are incorporated in the surface layer, increasing its protective effectiveness and consequently decreasing the corrosion rate.
4. Owing to the highly insulating character of rare earth oxides/hydroxides the barrier properties of the corrosion products layer are significantly enhanced. Moreover, the presence of lanthanide cations, RE^{3+}, entrapped as oxides/hydroxides in the surface layer is likely to exert an inhibiting action towards the corrosion process, thereby imparting active corrosion protection properties to the corrosion products layer.

REFERENCE

[1] K.U. KAINER, Magnesium – Alloys and Technology, Wiley-VCH Verlag Gmbh & Co. KgaA, Weinheim, 2003
[2] H.E. FRIEDRICH, B.L. MORDIKE, Magnesium Technology, Springer-Verlag, Berlin, Heidelberg, 2006
[3] M. POURBAIX, Atlas of Electrochemical Equilibria in Aqueous Solutions, 2nd ed., NACE, Houston, 1974
[4] G. SONG, A. ATRENS, Adv. Eng. Mater. 1 (1999) 11
[5] G. SONG, A. ATRENS, D. ST. JOHN, J. NAIRN, Y. LI, Corros. Sci. 39 (1997) 855
[6] G. SONG, A. ATRENS, D. ST. JOHN, X. WU, J. NAIRN, Corros. Sci. 39 (1997) 1981
[7] G. BARIL, N. PÉBÈRE, Corros. Sci. 43 (2001) 471
[8] G. SONG, A. ATRENS, X. WU, B. ZHANG, Corros. Sci. 40 (1998) 1769
[9] X.W. GUO, J.W. CHANG, S.M. HE, W.J. DING, X. WANG, Electrochim. Acta 52 (2007) 2570
[10] M.C. ZHAO, M. LIU, G. SONG, A. ATRENS, Adv. Eng. Mater. 10 (2008) 104
[11] Y.L. SONG, Y.H. LIU, S.R. YU, X.Y. ZHU, S.H. WANG, J. Mater. Sci. 42 (2007) 4435
[12] Y.L. SONG, Y.H. LIU, S.R. LIU, X.Y. ZHU, Mater. Corros. 58 (2007) 189
[13] A. PARDO, M.C. MERINO, A.E. COY, R. ARRABAL, F. VIEJO, E. MATYKINA, Corros. Sci. 50 (2008) 823
[14] M. ANIK, G. CELITKEN, Corros. Sci. 49 (2007) 1878
[15] A.M. LAFRONT, W. ZHANG, S. JIN, R. TREMBLAY, D. DUBÉ, E. GHALI, Electrochim. Acta 51 (2005) 489
[16] T. ZHANG, Y. SHAO, G. MENG, F. WANG, Electrochim. Acta 53 (2007) 561
[17] G. SONG, D. STJOHN, J. Light Metals 2 (2002) 1

[18] X.W. CHANG, P.H. FU, X.W. GUO, L.M. PENG, W.J. DING, Corros. Sci. 49 (2007) 2612
[19] F. ZUCCHI, V. GRASSI, A. FRIGNANI, C. MONTICELLI, G. TRABANELLI, J. Appl. Electrochem. 36 (2006) 195
[20] W. LIU, F. CAO, L. CHANG, Z. ZHANG, J. ZHANG, Corros. Sci. 51 (2009) 1334
[21] W. LIU, F. CAO, A, CHEN, L. CHANG, J. ZHANG, C. CAO, Corros. Sci. 52 (2010) 627
[22] W. LIU, F. CAO, B. JIA, L. ZHENG, J. ZHANG, C. CAO, X. LI, Corros. Sci. 52 (2010) 639
[23] G.L. SONG, Adv. Eng. Mater. 7 (2005) 563
[24] F. ROSALBINO, E. ANGELINI, S. DE NEGRI, A. SACCONE, S. DELFINO, Intermetallics 13 (2005) 55
[25] A.A. NAYEB-HASHEMI, J.B. CLARK, Phase diagrams of binary magnesium alloys, ASM International, Metals Park, Ohio, 1988
[26] F. EL-TAIB HEAKAL, A. FEKRY, M.Z. FATAYERJI, Electrochim. Acta 54 (2009)1545
[27] H. GAO, Q. LI, F.N. CHEN, Y. DAI, F. LUO, L.Q. LI, Corros. Sci. 53 (2011) 1401
[28] F. EL-TAIB HEAKAL, A.A. GHONEIM, A. FEKRY, J. Appl. Electrochem. 37 (2007) 405
[29] G.T. BURSTEIN, Corros. Sci. 47 (2005) 2858
[30] G. WU, Y. FAN, A. ATRENS, C. ZHAI, W. DING, J. Appl. Electrochem. 38 (2008) 251
[31] M. LIU, P. SCHMUTZ, S. ZANNA, A. SEYEUX, H. ARDELAN, G. SONG, A. ATRENS, P. MARCUS, Corros. Sci. 52 (2010) 562
[32] M. LIU, S. ZANNA, H. ARDELAN, I. FRATEUR, P. SCHMUTZ, G. SONG, A. ATRENS, P. MARCUS, Corros. Sci. 51 (2009) 1115
[33] G. SONG, A. ATRENS, Adv. Eng. Mater. 5 (2003) 837
[34] G. SONG, Adv. Eng. Mater. 7 (2005) 563
[35] G. SONG, A. ATRENS, Adv. Eng. Mater. 9 (2007) 177
[36] M.A. ARENAS, A. CONDE, J.J. DE DAMBORENEA, Corros. Sci. 44 (2002) 511
[37] A.M. CABRAL, W. TRABELSI, W. SERRA, M.F. MONTEMOR, A.L. ZHELUDKEVICH, M.G.S. FERREIRA, Corros. Sci. 48 (2006) 3740
[38] F. EL-TAIB HEAKAL, O.S. SHEATA, N.S. TANTAWY, Corros. Sci. 56 (2012) 86
[39] H. ARDELEAN, I. FRATEUR, P. MARCUS, Corros. Sci. 51 (2009) 3030
[40] A.L. RUDD, C. BRESLIN, F. MANSFELD, Corros. Sci. 42 (2000) 275
[41] G. MILAZZO, S. CAROLI, Tables of Standard Electrode Potentials,Wiley, New York, 1978
[42] P.L. MILLER, B.A. SHAW, R.G. WENDT, W.C. MOSHIER, Corrosion 51 (1995) 922
[43] H.B. YAO, Y. LI, A.T.S. WEE, Electrochim. Acta 48 (2003) 4197